PREDICTION OF STRAND FEEDSTOCK MECHANICAL PROPERTIES WITH NEAR INFRARED SPECTROSCOPY

Neil J. Kohan,[a] Brian K. Via,[a,b,c]* and Steven E. Taylor [b,c]

Wood strands either prepared in the laboratory or from a manufacturing plant were assessed for their ultimate tensile strength, tensile MOE, bending strength, and bending stiffness, and then near infrared spectroscopy was utilized for prediction. The ability to predict ultimate tensile strength and stiffness was generally weaker than bending strength and stiffness, perhaps due to the homogeneous distribution of stresses that occur within the strand during 3-point bending. Prediction of ultimate tensile strength and elasticity of plant based strands were generally weak due to imperfections in the strands that originate during biomass breakdown; however, for laboratory strands, prediction of tensile strength and stiffness was moderate/better. The modulus of elasticity for strands under bending exhibited the strongest correlation (R^2 = 0.76). Principal component loadings were assessed, and it was found that the cellulose crystalline- and semi-crystalline-associated wavelengths were most important in predicting the stiffness for both tensile and bending forces; however, the influence of lignin-associated wavelengths increased in importance when predicting bending strength, and it was hypothesized that this was attributable to the plastic response of lignin above the proportional limit in the stress-to-strain curve. This study demonstrates the potential of near infrared spectroscopy to monitor the biomass quality prior to composite manufacture.

Keywords: NIR; Spectroscopy; Wood; Composite; OSB; Strength; Stiffness; Biomass; Feedstock

Contact information: a: Biomaterials Laboratory, School of Forestry and Wildlife Sciences, 3301 Forestry and Wildlife Sciences Building, Auburn, AL 36849-5418 US; b: Department of Biosystems Engineering, 214 Corley Building, Auburn University, Auburn, AL 36849-5417 USA; c: Center for Bioenergy and Bioproducts, 520 Devall Drive, Auburn University, Auburn, AL 36849;
** Corresponding author: bkv0003@auburn.edu*

INTRODUCTION

The goal of engineered wood composites is to design biomaterials that achieve more uniformity in performance attributes such as strength and dimensional stability. Furthermore, in the southern United States, wood strand composite manufacturers seek to utilize strands from smaller diameter pine trees that are not always suitable for structural lumber or veneer due to higher concentrations of juvenile wood. The higher concentration of juvenile wood can result in lower modulus of elasticity (MOE) in wood composites with high alignment coupled with a higher surface-to-core ratio. Ways to monitor the feedstock prior composite manufacture could be useful to determine whether strands could be used for higher value composites or for other uses such as commodity biofuels (Ragauskas *et al.* 2006; Via 2010; Via *et al.* 2011).

Near infrared reflectance spectroscopy (NIRS) is a known method for rapid nondestructive analysis of both the physical and mechanical properties of wood, and it may be useful for monitoring the quality of the biomaterial. For example, NIRS has been useful in prediction of mechanical properties of lumber when compared to visual-based grading (Hoffmeyer and Pedersen 1995). Others have demonstrated the ability of NIRS to monitor the bending strength and MOE for radiata pine (*Pinus radiata*) for samples moving at 900 mm/min (Thumm and Meder 2001). Gindl *et al.* (2004) performed similar tests on clear samples of European larch, and they found that the mechanical properties of samples with compression wood could be predicted with NIRS spectra (Gindl *et al.* 2004). Other studies have even suggested that measurement of microfibril angle appears possible (Jones *et al.* 2005), and this is probably due to the relationship of microfibril angle to the underlying chemistry matrix within the woody cell wall due to the change in fiber morphology with chemistry in the radial plane of the tree stem (Gindl *et al.* 2001; 2007, 2009). Kelley *et al.* (2004) used NIRS to investigate the physical and mechanical properties of loblolly pine (*Pinus taeda*). Samples were analyzed using both full-range (500 to 2500 nm) and limited-range (650 to 1150 nm) spectra. Results from full and reduced range were similar, with a maximum R^2=0.88 for MOE. Via *et al.* (2003) used NIRS to model the strength and stiffness of longleaf pine (*Pinus palustris*), using clear samples and both multiple linear regression (MLR) and principal component regression (PCR). They observed that NIRS models built from mature wood spectra were not suitable for predicting mechanical properties of juvenile wood. In 2005, Via *et al.* investigated the ability to use NIRS for southern yellow pine species in the presence of blue stain. It was found that models could be built that were insensitive to blue stain sensitive wavelengths, but differences in NIR spectrometers can introduce bias and a reduction in model precision (Via *et al.* 2005).

For wood-based strands, tensile testing is often utilized to characterize the strength of the wood feedstock prior to manufacture. But specimen geometry and gauge length can impact the accuracy of the reading, and test setup should be considered, given the lack of ASTM standards (Kohan *et al.* 2012). For plant-based strands, imperfections during stranding can confound the accuracy; on the other hand, this may be more representative of real strands utilized in industry.

To date, very little research has occurred involving the prediction of the tensile mechanical properties of wood using NIRS. Tsuchikawa *et al.* (2005) investigated NIRS and tensile properties in 2005 using Japanese species. Tensile tests were conducted according to Japanese Industrial Standards, and the study yielded an R^2 = 0.53 to 0.74 for tensile MOE and 0.44-0.74 for ultimate tensile strength (UTS). The tensile test may be useful due to the sensitivity of wood UTS to the angle and concentration of wood polymers, while the bending test, which includes tension and compression forces, is more often utilized in the literature.

The objective of this study was to characterize the ability of NIRS in the prediction of the UTS, tensile MOE, bending modulus of rupture (MOR), and bending MOE of wood strands characteristic of those used in wood strand composites, such as oriented strand board and oriented strand lumber. Plant and laboratory prepared strands were tested to determine which could be used in the calibration of NIRS.

EXPERIMENTAL

Materials

All wood strands utilized were identified as southern yellow pine (*Pinus* spp.). Plant strands were obtained from a local oriented strand board (OSB) plant. Flakes were collected from the manufacturing line just before the screening zone. Sawn strands were produced from cut-offs which were short (0.3 to 0.6 meters). The cut-offs were donated by a local truss plant, and the boards were purchased locally. Different sources of wood were selected to ensure a wide range in mechanical and physical properties by observing the latewood percentage on the cross section. Boards and cut-offs were cut into clear samples 25 mm by 25 mm by 200 mm in length and placed in the humidity chamber at 22°C and 50% relative humidity. The samples were allowed to equilibrate prior to processing and/or testing.

Plant strands to be used for calibration were sorted from approximately 1.3 cubic meters of unscreened strands. Radially-cut strands with dimensions of at least 125 mm in length and 25 mm in width were selected. Strands with splitting or warp (bends, twists, cupping) were not selected. The selected strands were then cut to a uniform size using a guillotine paper cutter. To produce sawn strands, the collected lumber cut-offs were first cut into small clear samples measuring 200 x 25 x 25 mm. These small clear samples were then ripped along the radial face to produce strands of approximately 200 x 25 x 1.0 mm. Both plant and sawn strands were returned to the humidity chamber and were reconditioned at 22°C and 50% relative humidity until they reached weight equilibrium. A total of 150 plant strands were tested: 70 tension samples and 80 bending samples. A total of 100 sawn strands were tested: 50 in tension, and 50 in bending.

Near Infrared Spectroscopy

A Perkin Elmer Spectrum 400 FT-IR/FT-NIR Spectrometer was used to collect the NIR spectra from the radial face with the smoothest surface used for spectra collection. Since the thickness of the samples were 1.0 mm, it was assumed that the wood chemistry on both faces were equal. Absorbance was recorded from 1000 to 2500 nm with resolution of 0.5 nm. Spectra were produced for four equidistant locations from the center (square pattern – approximately 15 mm between each point), with each spectrum composed of eight individual scans with a beam diameter of approximately 7 mm. The four individual spectra for each strand were averaged using Spectrum 6.2 software to produce one average spectrum for each wood strand.

The raw NIR spectra baseline can be offset to zero, so the 1^{st} and 2^{nd} derivative was applied as a pretreatment (30 point segment size) to determine if improvements in precision could be made.

Mechanical Testing

Both axial tension and bending tests were conducted on the wood strands using a Zwick-Roell load frame equipped with 10 kN load cell and a computer-controlled screw-drive crosshead. Tensile testing was conducted using screw type grips with a loading rate of 0.254 mm/min, a gage length of 50.8 mm (Epsilon Corp clip-on extensometer), and grip to grip separation of 76.2 mm. Tensile samples exhibiting grip type failures or any

failure outside of the gage length were not included in the analysis. Bending tests were conducted in three-point setup with a loading rate of 4.0 mm/min, and support separation of 75 mm for sawn strands and 50 mm for plant strands.

Chemometric Modeling

Following mechanical testing multiple linear regression (MLR) and principal components regression (PCR) models were created using Quant+ software package. The Quant+ software allowed for spectra pretreatment by taking the first and second derivatives of absorption in addition to the raw spectra. Models were developed for tensile modulus (MOE), ultimate tensile strength (UTS), bending modulus of elasticity (MOE), and modulus of rupture (MOR). Calibrations were estimated using full-cross validation. Mechanical testing results and spectra were also exported to Microsoft Excel for averaging and interpretation.

Principal components regression (PCR) and Multiple Linear Regression (MLR) models were produced using Perkin Elmer Spectrum Quant+ software package. Separate models were developed for raw and pretreated spectra.

RESULTS AND DISCUSSION

Results for statistical models for the tensile tests are displayed in Table 1, and bending model results are shown in Table 2. A baseline correction of NONE represents the raw spectra, while $dA/d\lambda$ and $d^2A/d\lambda^2$ represent first and second derivative pretreated spectra. PC is the number of principle components or factors used in the model (each factor generally corresponds to one or more spectral peaks). The coefficient of calibration (R^2) represents the proportion of property variability accounted for in the model. The ratio of performance to deviation (RPD) is a general indicator of model predictive adequacy while the standard error of calibration (SEC) is used to access model fit to the data (Bailleres *et al*. 2002). RPD is calculated as standard deviation divided by standard error of prediction (SEP).

Table 1. Principal Component and Multiple Linear Regression Models for Raw, 1st, and 2nd Derivative Spectra for Samples Loaded in Tension

Type	Property	Baseline Correction	Model Type	Factors	R^2	SEC	SEP	RPD
Plant	MOE	NONE	MLR	9	0.26	2.78	3.36	0.862
(n=70)	UTS	NONE	MLR	9	0.37	13.97	16.78	0.957
Plant	MOE	$d^2A/d\lambda^2$	PCR	7	0.13	2.90	3.41	0.830
(n=70)	UTS	$d^2A/d\lambda^2$	MLR	7	0.30	14.33	16.59	0.931
Sawn	MOE	NONE	MLR	5	0.61	2.05	2.56	1.069
(n=50)	UTS	NONE	MLR	5	0.37	17.98	21.33	0.889
Sawn	MOE	$d^2A/d\lambda^2$	MLR	4	0.55	2.19	2.47	1.218
(n=50)	UTS	$d^2A/d\lambda^2$	MLR	4	0.46	10.59	10.99	1.167

Table 2. Principal Component Models for Raw and 1st Derivative Spectra for Samples Loaded in Bending

Type	Property	Baseline Correction	Model Type	Factors	R^2	SEC	SEP	RPD
Plant (n=80)	MOE	NONE	PCR	8	0.48	0.894	1.065	1.07
	MOR	NONE	PCR	5	0.43	12.8	15.3	1.05
Plant (n=80)	MOE	dA/dλ	PCR	6	0.50	0.846	0.939	0.84
	MOR	dA/dλ	PCR	3	0.35	13.6	16.0	1.02
Sawn (n=50)	MOE	NONE	PCR	5	0.75	0.624	0.777	1.54
	MOR	NONE	PCR	2	0.45	12.3	13.3	1.22
Sawn (n=50)	MOE	dA/dλ	PCR	6	0.76	0.621	0.805	1.48
	MOR	dA/dλ	PCR	3	0.51	11.7	13.9	1.16

The strongest models for plant strand MOE and UTS were achieved using raw spectra, producing coefficients of determination of 0.26 for MOE and 0.37 for UTS. Likewise, the highest RPD for MOE and UTS were achieved using raw spectra (Table 1). Actual versus predicted plots are shown in Fig. 1.

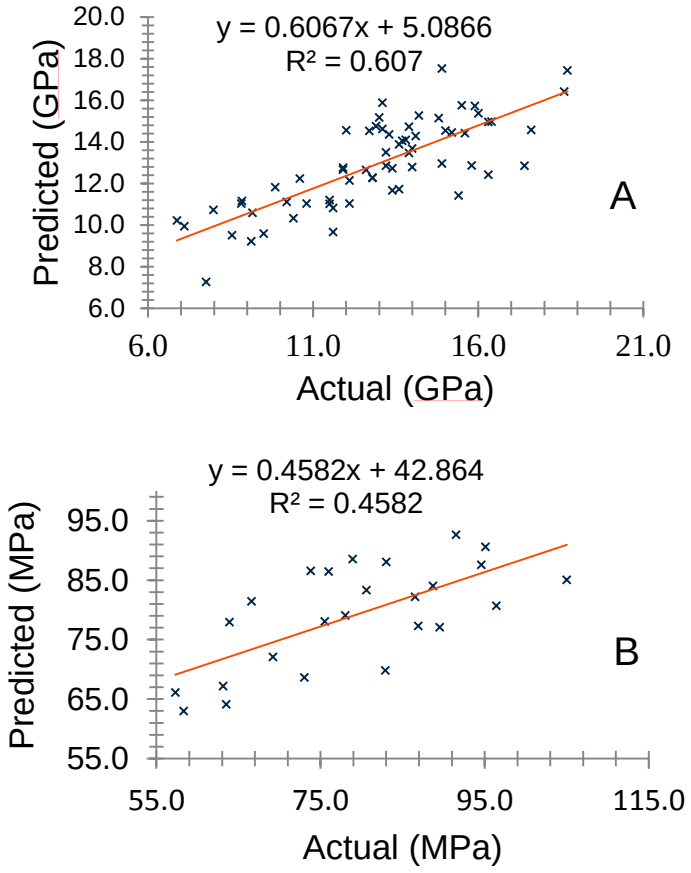

Fig. 1. Tensile Testing: Actual Values versus NIRS Predicted Values for (a) MOE and (b) UTS for sawn strands

The best MOE predictive model was built using the raw spectra, which yielded a coefficient of determination of 0.61. For UTS, the second derivative spectra yielded better results than the raw spectra, with an R^2 of 0.46. For both MOE and UTS, the highest RPD values were reached using second derivative spectra. The models compare well with existing NIRS and tensile testing research that has produced R^2 values ranging from 0.53 to 0.74 for MOE using samples from one board (Tsuchikawa *et al.* 2005). The best models for MOE were produced using the second derivative spectra, which removes baseline shift associated with density. Since the models were linear in nature, removing density as a factor may better predict tensile MOE as the relationship between tensile MOE and density is nonlinear (Biblis 1969).

Models produced from the spectra and flexural properties were significantly better than the tensile models (Fig. 2A and B). The better predictability was the result of consistent and predictable failure location achieved through flexural testing. Furthermore, flexural testing takes into account the entire cross section of the sample, whereas tensile testing results are more dependent on the weakest portion of a material that is anisotropic and nonhomogenous. That is to say, a single point of weakness, such as a severed tracheid or local area of low density, will greatly reduce the ability of a sample to carry proportional loads, leading to premature failure (Biblis 1969).

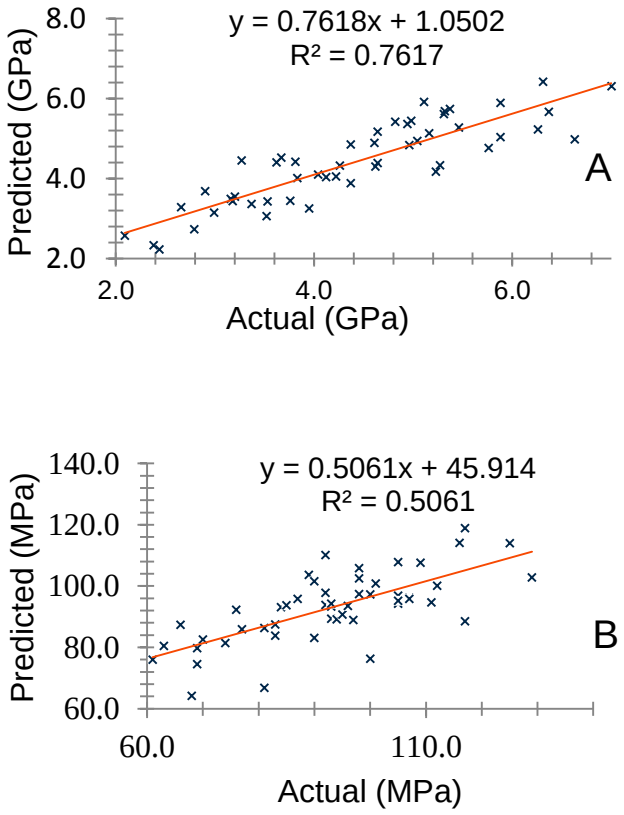

Fig. 2. Bending Testing: Actual Values versus NIRS Predicted Values for (a) MOE and (b) MOR for sawn strands

As with the tensile models, the flexural models performed better for sawn strands than plant strands. This is most likely the result of manufacturing defects present in plant strands that are not present in sawn strands. The strongest model for MOE of plant strands was created using the first derivative of the spectra, with an R^2 value of 0.50. The strongest MOR model for plant strands was created using raw spectra with R^2 of 0.43. The best calculated RPD for plant models were 0.84 for MOE and 1.05 for MOR. With sawn strand samples the models for MOE and MOR were strongest using first derivative spectra, with an R^2 of 0.76 for MOE and an R^2 of 0.51 for MOR. RPD values for MOE and MOR were 1.48 and 1.16, respectively (Table 2).

Interpretation

For interpretation of key spectroscopic features important in the prediction of mechanical properties, regression of Principal Components (PCs) (as independent variables) were produced from PCR analysis to predict the strength and stiffness of strands in tension and bending. Key wavelengths are labeled in Fig. 3 according to the index number given in Table 3.

Table 3. Assignment of Absorption Bands to Important Wood Chemistry Constituents (Schwanninger *et al.* 2011)

Index Number	Wavelength (nm)	Polymer/Chemistry Assignment
1	1130-1135	Aromatic portion of lignin
2	1423-1428	Amorphous region of cellulose
3	1476	Semi-crystalline regions of cellulose
4	1548-1592	C3-C5 intramolecular bond, Crystalline regions of cellulose
5	1672	Aromatic portion of lignin
6	1724	Furanose/pyranose due to hemicellulose
7	1758	Alpha cellulose
8	1790-1830	Semi-crystalline or crystalline regions of cellulose
9	2080	Semi-crystalline or crystalline regions of cellulose
10	2140	Amorphous regions of cellulose
11	2200	C-H and C=O stretch in lignin
12	2336	Semi-crystalline regions of cellulose, hemicelluloses, and xylan

In the regression spectrum for tensile MOE of sawn strands, key wavelengths associated with cellulose were most dominant (Fig. 3A). Wavelengths for the crystalline regions of cellulose (4) and semi-crystalline or crystalline regions of cellulose (8, 9, 10, 12) were most dominant, which is probably attributable to the shear forces at the C3-C5 hydrogen bonds (Winandy and Rowell 1984). Furthermore, the strong presence of lignin (5) and amorphous cellulose regions (3), are in agreement with the findings of Tsuchikawa *et al.* (2005).

The regression coefficients for UTS were generally similar to the regression spectrum for MOE in tension (Fig. 3A and B). However, relative to other wavelengths, peak 5, which was attributable to the aromatic portion of lignin, was slightly more critical for prediction of UTS.

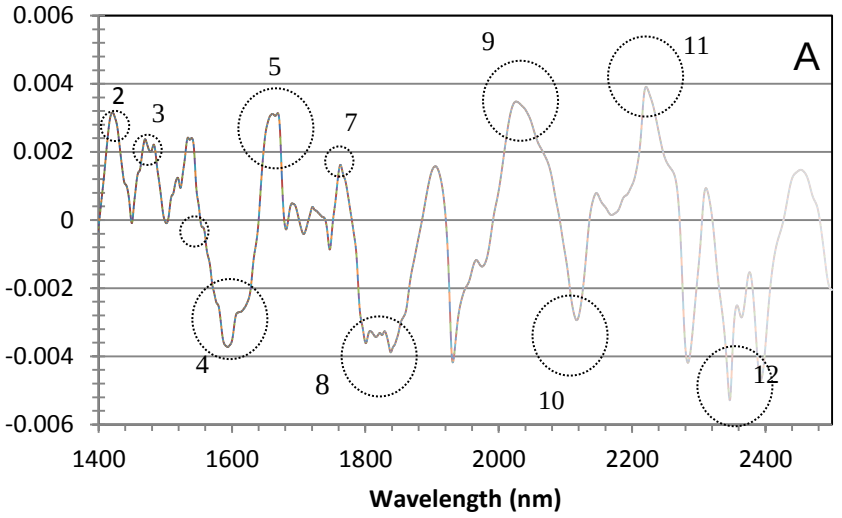

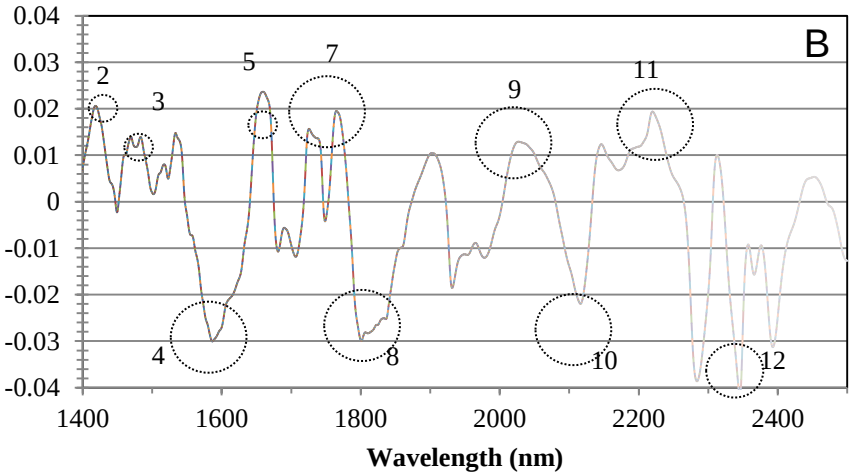

Fig. 3. Regression spectrum for tensile models for (a) MOE and (b) UTS of sawn strands. The regression spectrum was based on 1000 to 2500 nm, but only the relevant wavelength range is shown

This was explained by Via *et al.* (2009), in which the plasticity of lignin above the proportional limit, for wood samples in bending, probably played an increased role in the strength of the material, particularly for high microfibril angles in which the forces on the lignin matrix are in series. However, in that study, multiple linear regression was used to normalize the effect of microfibril angle prior to lignin wavelength assessment, resulting in a better ability to see trends. The microfibril angle could not be measured in this study but probably is non-linearly related to the lignin concentration in the S2 layer and is an important component in the tensile strength of wood (Hein and Brancheriau 2011; Via *et al.* 2007).

In the flexural MOE regression spectrum, wavelengths corresponding to cellulose (2, 4, 7, 9, 10, 12), hemicellulose (6), and lignin (1, 5) were present (Fig.4 A). The most dominant wavelengths in the MOE regression spectrum were those attributable to crystalline cellulose (4) and semi-crystalline or crystalline regions of cellulose (12). This supports the theory of others in which cellulose is the dominant polymer in wood stiffness below the elastic limit (Winandy and Rowell 1984). The presence of alpha cellulose related wavelength (7) concurs with the findings of Via *et al.* (2009), who found alpha cellulose to be an important factor for prediction of MOE and MOR for solid wood in bending. Also in this study, the regression spectra for flexural MOE was built using PCR, and hemicellulose associated wavelengths (6) were found to be important factors. This is in agreement with others who found hemicellulose to be an important factor for MOE when using PCR models (Via *et al.* 2009).

Beyond the elastic limit in flexure, hemicellulose and lignin polymers are expected to resist stresses as they are transferred from cellulose microfibrils to the surrounding hemicellulose-lignin matrix. As a result, cellulose-related wavelengths (2, 3, 4, 8, 10, 12) remain important, but lignin-related wavelengths (1) become more important than under purely elastic circumstances (Fig. 4B). Alpha cellulose related wavelengths (7) were not as important, and this is attributable to the presence of juvenile wood samples in the prediction model. Furthermore, hemicellulose-related wavelengths (6) were not particularly important for MOR models in this study and others (Via *et al.* 2009). The high importance of the aromatic portion of lignin (1) was also in agreement with other studies (Via *et al.* 2009).

It is interesting to note that alpha-cellulose-related wavelengths (2) were more pronounced in the MOR regression spectrum than in the MOE regression spectrum. Although it is known that the crystalline regions are stiffer than the amorphous regions, the plastic response of amorphous cellulose is not fully understood (Keckes *et al.* 2003). However, the presence of amorphous cellulose-related wavelengths in the MOR regression spectra indicates that the amorphous region of cellulose plays a significant role in the plastic response of wood.

Finally, it should be noted that PCR analysis for MOR modeling was utilized to provide some insight about the possible relationship between the plastic response of lignin to forces that occur beyond the proportional limit. However, to better test this hypothesis, future work should focus on the collection of spectra from both the compression and tension side of the specimen in both the elastic and plastic region of the stress-to-strain curve.

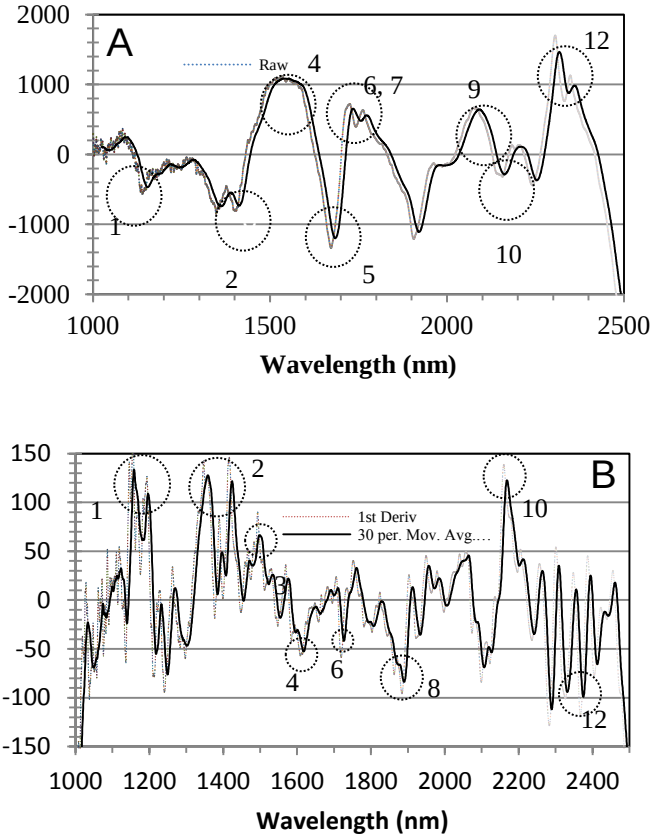

Fig. 4. Regression spectrum for flexural models (a) MOE unprocessed spectra and (b) MOR after preprocessing for 1st derivative and 30 point moving average for smoothing for sawn strands.

CONCLUSIONS

1. The ability to predict the mechanical properties of wood strands fell in the following order: MOE bending sawn strand ($R^2 = 0.76$) > MOE tension sawn strand ($R^2 = 0.61$) > MOR bending plant strand ($R^2 = 0.51$) > UTS tension plant strand ($R^2 = 0.46$).
2. The cellulose crystalline- and semi-crystalline-associated wavelengths were the most important in predicting the stiffness for both tensile and bending forces.
3. Lignin-associated wavelengths, while important for stiffness, were also important when predicting bending strength.
4. Prediction of strands from an industrial plant was difficult, and sawing samples in the lab may be preferred, depending on the application of NIRS.

ACKNOWLEDGMENTS

The authors are grateful for the funding support provided by McIntire-Stennis and HATCH and would like to note that this research is specifically in alignment with PROJ NO: ALAZ00051 McIntire Stennis, PROJ NO: ALA0TAYLOR HATCH, and PROJ NO: ALA031-1-09020. The authors would like to also thank the Center for Bioenergy and Bioproducts for allowing the use of their laboratory facilities during the conditioning and scanning of the strands. This project was in alignment with the Center for Bioenergy and Bioproducts and the Forest Products Development Center, in which there is an interest in characterizing the feedstock for value added opportunities.

REFERENCES CITED

Bailleres, H., Davrieus, F., and Pichavant, F. H. (2002). "Near infrared analysis as a tool for rapid screening of some major wood characteristics in a eucalyptus breeding program," *Ann. for Sci.* 59(5-6), 479-490.

Biblis, E. J. (1969). "Transitional variation and relationships among properties within loblolly pine growth rings," *Wood Sci. Technol.* 3(1), 14-24.

Gindl, W., Gupta, H. S., Schoberl, T., Lichtenegger, H. C., and Fratzl, P. (2004). "Mechanical properties of spruce wood cell walls by nanoindentation," *Appl. Phys. A-Mater.* 79(8), 2069-2073.

Gindl, W., Teischinger, A., Schwanninger, M., and Hinterstoisser, B. (2001). "The relationship between near infrared spectra of radial wood surfaces and wood mechanical properties," *J. Near Infrared Spec.* 9(4), 255-261.

Hein, P. R. G., and Brancheriau, L. (2011). "Radial variation of microfibril angle and wood density and their relationships in 14-year-old eucalyptus urophylla st blake wood," *BioResources* 6(3), 3352-3362.

Hoffmeyer, P., and Pedersen, J. G. (1995). "Evaluation of density and strength of Norway spruce wood by near-infrared reflectance spectroscopy," *Holz Als Roh- und Werkstoff* 53(3), 165-170.

Jones, P. D., Schimleck, L. R., Peter, G. F., Daniels, R. F., and Clark III, A. (2005). "Nondestructive estimation of *Pinus taeda* L. Wood properties for samples from a wide range of sites in georgia," *Can. J. Forest Res.* 35(1), 85-92.

Keckes, J., Burgert, I., Fruhmann, K., Muller, M., Kolln, K., Hamilton, M., Burghammer, M., Roth, S. V., Stanzl-Tschegg, S., and Fratzl, P. (2003). "Cell-wall recovery after irreversible deformation of wood," *Nat. Mater.* 2(12), 810-814.

Kelley, S. S., Rials, T. G., Snell, R., Groom, L. H., and Sluiter, A. (2004). "Use of near infrared spectroscopy to measure the chemical and mechanical properties of solid wood," *Wood Sci. Technol.* 38(4), 257-276.

Kohan, N., Via, B.K., and Taylor, S. (2012). " A Comparison of Geometry Effect on Tensile Testing of Wood Strands," *Forest Prod. J.* Page numbers to be assigned.

Ragauskas, A. J., Williams, C. K., Davison, B. H., Britovsek, G., Cairney, J., Eckert, C. A., Frederick, W. J., Hallett, J. P., Leak, D. J., Liotta, C. L., Mielenz, J. R., Murphy,

R., Templer, R., and Tschaplinski, T. (2006). "The path forward for biofuels and biomaterials," *Science* 311(5760), 484-489.

Schwanninger, M., Rodrigues, J., and Fackler, K. (2011). "A review of band assignments in near infrared spectra of wood and wood components," *Journal of Near Infrared Spectroscopy* 19, 287-308.

Thumm, A., and Meder, R. (2001). "Stiffness prediction of radiata pine clearwood test pieces using near infrared spectroscopy," *Journal of Near Infrared Spectroscopy* 9(2), 117-122.

Tsuchikawa, S., Hirashima, Y., Sasaki, Y., and Ando, K. (2005). "Near-infrared spectroscopic study of the physical and mechanical properties of wood with meso- and micro-scale anatomical observation," *Appl. Spectrosc.* 59(1), 86-93.

Via, B. K. (2010). "Prediction of oriented strand board wood strand density by near infrared and fourier transform infrared reflectance spectroscopy," *Journal of Near Infrared Spectroscopy* 18(6), 491-498.

Via, B. K., Fasina, O., and Pan, H. (2011). "Assessment of pine biomass density through mid-infrared spectroscopy and multivariate modeling," *BioResources* 6(1), 807-822.

Via, B. K., Shupe, T. F., Groom, L. H., Stine, M., and So, C. L. (2003). "Multivariate modelling of density, strength and stiffness from near infrared spectra for mature, juvenile and pith wood of longleaf pine (pinus palustris)," *Journal of Near Infrared Spectroscopy* 11(5), 365-378.

Via, B. K., So, C. L., Groom, L. H., Shupe, T. F., Stine, M., and Wikaira, J. (2007). "Within tree variation of lignin, extractives, and microfibril angle coupled with the theoretical and near infrared modeling of microfibril angle," *Iawa Journal* 28(2), 189-209.

Via, B. K., So, C. L., Shupe, T. F., Eckhardt, L. G., Stine, M., and Groom, L. H. (2005). "Prediction of wood mechanical and chemical properties in the presence and absence of blue stain using two near infrared instruments," *Journal of Near Infrared Spectroscopy* 13(4), 201-212.

Via, B. K., So, C. L., Shupe, T. F., Groom, L. H., and Wikaira, J. (2009). "Mechanical response of longleaf pine to variation in microfibril angle, chemistry associated wavelengths, density, and radial position," *Compos Part a-Appl. S.* 40(1), 60-66.

Winandy, J. E., and Rowell, R. M. (1984). "The chemistry of wood strength," *Adv. Chem. Ser.* (207), 211-255.

Article submitted: March 12, 2012; Peer review completed: April 29, 2012; Revised version accepted: May 20, 2012; Published: May 24, 2012.